RSC Advances

ROYAL SOCIETY OF CHEMISTRY

www.rsc.org/advances

Cite this: DOI: 10.1039/c0xx00000x

www.rsc.org/xxxxxx

COMMUNICATION

Spin crossover-graphene nanocomposites: facile syntheses, characterization, and magnetic properties

Dan Qiu,[a] Dong-Hong Ren,[a] Ling Gu,[a] Xiao-Li Sun,[a] Ting-Ting Qu,[a] Zhi-Guo Gu,[*a,b] and Zaijun Li[a]

Received (in XXX, XXX) Xth XXXXXXXXX 20XX, Accepted Xth XXXXXXXXX 20XX

DOI: 10.1039/b000000x

A facile way to fabricate spin crossover-graphene nanocomposites has been developed, and $[Fe(Htrz)_2(trz)](BF_4)$-graphene (SCO-G) nanocomposites have been successfully synthesized and characterized. SEM and TEM demonstrated that $[Fe(Htrz)_2(trz)](BF_4)$ nanoparticles (ca. 50 nm) distributed uniformly onto the surface of the graphene. Interestingly, graphene as a substrate produced an effect on the spin crossover properties of $[Fe(Htrz)_2(trz)](BF_4)$ nanoparticles.

The special phenomenon of spin crossover (SCO) between high-spin (HS) and low-spin (LS) states of electronic configurations from d^4 to d^7 has attracted extensive attention for its promising applications in sensors, displays, memories and molecular switches.[1] It is well known that the spin state of SCO compounds can be switched by external stimuli such as temperature change, light irradiation, the application of pressure, magnetic fields and so on.[2] Among SCO compounds, the triazole-based polymeric compounds aroused particular interests, which was attributed to the large hysteresis above room temperature and an obvious pink-to-white colour changes as it converted LS into HS state.[3] In particular, with the advent of nanotechnology, a variety of methods have been applied to successfully elaborate nanoparticles (NPs), thin films, or nano-patterned nanostrcutures of SCO complexes.[4] In addition, triazole-based polymeric SCO compounds were easy to fabricate nano-sized materials for investigating their size-dependent magnetic properities and possible applications in future nanophotonic, nanoelectronic and spintronic devices.[5] Furthermore, multifunctional SCO nanocomposites integrating the SCO functionality and other special properties have been synthesized by embedding SCO NPs into templates, such as organic polymers, biomolecular templates and silica matrices.[6]

Recently, the graphene and graphene-based materials have risen great interests because of their unique structure and specific properties within a single sheet of sp^2-bonded carbon atoms.[7] Graphene is well known as a two-dimensional carbon substrate, which could be used for the deposition of inorganic NPs owing to its high specific surface area (2630 m^2 / g).[8] The past numerous reports have demonstrated that incorporation of nanomaterials with graphene could generate new materials exhibiting each component, or even with a synergetic effect, which holds great promise on fabricating enhanced chemical- sensing platforms.[9] In recent years, much efforts have been made to develop graphene-metal oxide and graphene-metal nanocomposites with different morphologies for applications in catalysis, energy devices and optoelectronic materials.[10] Metal-organic frameworks (MOFs), a new class of functional materials, combined with graphite oxide have been reported to exhibit exceptional properties for adsorption and catalyst.[11] However, to the best of our knowledge, there is no attempt to prepare SCO-graphene nanocomposites. Decorating SCO nanoparticles on graphene will impart the SCO-G nanocomposites spin crossover properties and favourable electro transfer, which may make the composite materials promising for applications in data-storage and spintronic devices.

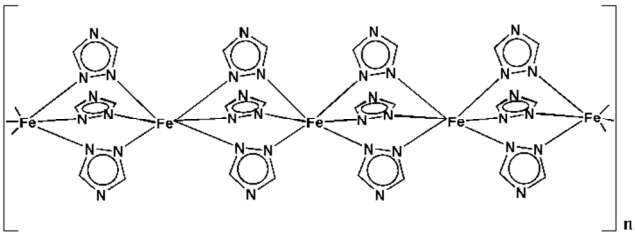

Fig. 1 Molecular structure of the polynuclear complexes of iron (II) with 1, 2, 4- triazoles.

In order to design and manufacture SCO-G nanocomposites, it is crucial to select the spin-crossover compounds by considering its stability, magnetic properties, and the tailored nanometer scale structures. $[Fe(Htrz)_2(trz)](BF_4)$ (Htrz = 1H-1,2,4-triazole), one of the most standout SCO compounds with 1D polymeric structure by binding Fe(II) ions with 1,2,4-triazole ligands (Fig. 1), was first applied to fabricate SCO-graphene nanocomposites by a facile two steps in this paper. The preparation of the pure SCO NPs was achieved according to a recent reverse-micelle technique with appropriate modifications (see detailed synthesis in the SI). Briefly, the SCO NPs were synthetized by adding triazole aqueous solution into a water-in-oil microemulsion including $Fe(BF_4)_2{\cdot}6H_2O$ salt. In comparison with the reported method of mixing the triazole ligand microemulsion and the iron(II) salts microemulsion,[3] our fabrication strategy used only one microemulsion that triazole permeated in the microemulsion droplets and reacted with $Fe(BF_4)_2{\cdot}6H_2O$ through solubilization, and thus favored the nucleation and growth of SCO NPs. The SCO NPs were then simply deposited on the surface of graphene by supersonic in ethanol with different mass ratios of SCO NPs to

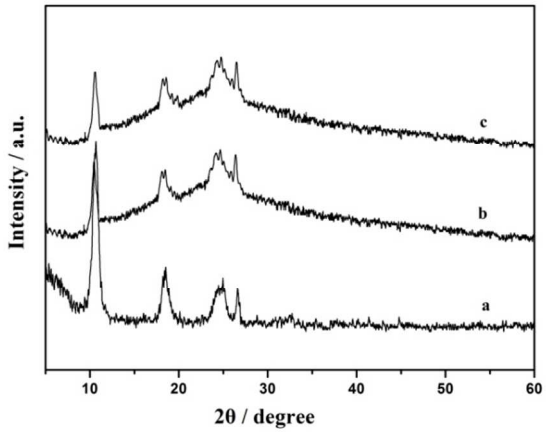

Fig. 2 X-ray diffraction patterns of $[Fe(Htrz)_2(trz)](BF_4)$ (a), SCO-G1 (b) and SCO-G2 (c).

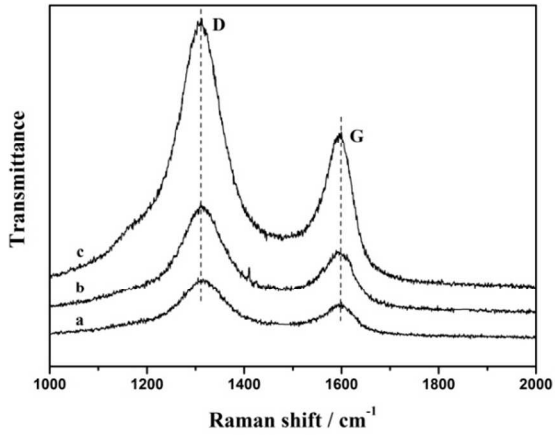

Fig. 3 Raman spectra of SCO-G1 (a), SCO-G2 (b), Graphene (c).

graphen. The resulting nanocomposites SCO-G1 (SCO:graphen mass ratio 2:1) and SCO-G2 (SCO:graphen mass ratio 3:5) were investigated to demonstrate the effect of graphene on the spin-crossover properties of the nanocomposites.

X-ray powder diffraction measurements were employed to investigate the phase and structure of the synthesized SCO-G nanocomposites. As shown in Fig. 2, the observed diffraction patterns at 2θ values of about 10°, 18°, 24° and 26° for SCO-G and the pure $[Fe(Htrz)_2(trz)](BF_4)$ NPs, matched well the peaks of the reported $[Fe(Htrz)_2(trz)](BF_4)$ microcrystalline material.[3, 12] It suggested that the $[Fe(Htrz)_2(trz)](BF_4)$ NPs were successfully prepared, and their crystalline structures were maintened in the SCO-G nanocomposites, which were confirmed by FT-IR and TGA (ESI†). Compared with the pure $[Fe(Htrz)_2(trz)](BF_4)$ NPs, the broad peaks in the range of 15-35° of SCO-G nanocomposites corresponded to the reflection of graphene around at 25°, indicating that the graphene might stack in the reaction process and disorder along the stacking direction.[13]

Raman spectra of the original graphene and the resulting SCO-G nanocomposites can provide informations about the structure changes during the deposition of $[Fe(Htrz)_2(trz)](BF_4)$ NPs on the surface of graphene. As shown in Fig. 3, the spectra of all the samples exhibited two strong bands at ca. 1312 and 1599 cm^{-1}, which corresponded to D band related to the presence of disordered defects in the graphite and G band assigned to the in-plane vibration of graphite lattice, respectively.[14] The Raman area ratios of D and G bands of SCO-G1 (2.68) and SCO-G2 (2.63) were larger than graphene (2.60), which could be attributed to a partially ordered crystal structure and the presence of some unrepaired defects of graphene during the fabrication process of SCO-G nanocomposites.[15]

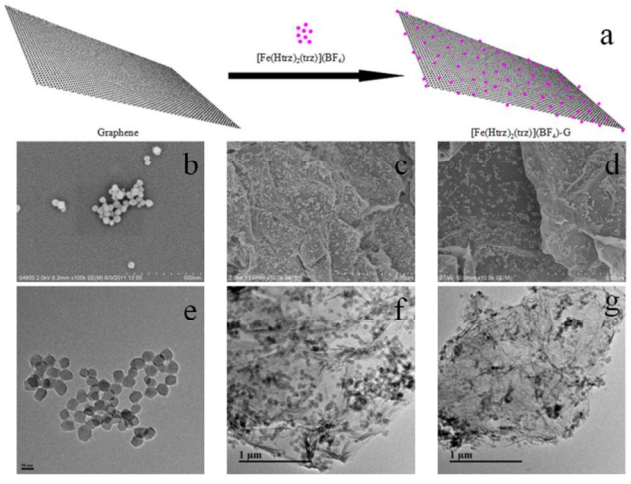

Fig. 4 Schematic illustration of the formation of SCO-G (a); SEM images of $[Fe(Htrz)_2(trz)](BF_4)$ (b), SCO-G1 (c), SCO-G2 (d); TEM images of $[Fe(Htrz)_2(trz)](BF_4)$ (e), SCO-G1 (f), SCO-G2 (g).

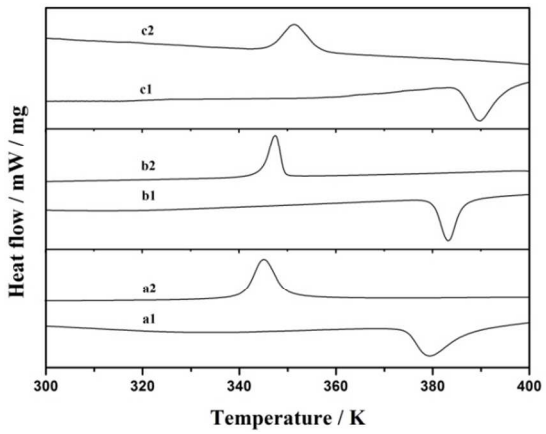

Fig. 5 DSC curves of $[Fe(Htrz)_2(trz)](BF_4)$ (a1 heating, a2 cooling), SCO-G1 (b1 heating, b2 cooling), SCO-G2 (c1 heating, c2 cooling).

The electron microscopy measurements provided an external direct-viewing impression of SCO-G nanocomposites. As shown in Fig. 4b and Fig. 4e, the pure $[Fe(Htrz)_2(trz)](BF_4)$ NPs exhibited regular ball-like shape with an average size of ca. 50 nm. In the SEM images of SCO-G (Fig. 4c and 4d), the large graphene flakes exhibited slightly wrinkled surface, and the edge of the films showed a layered structure of stacked thin graphene sheets, from which $[Fe(Htrz)_2(trz)](BF_4)$ NPs could be observed as bright dots on both sides of graphene. The phenomenon suggested that the SCO NPs were deposited on both sides of graphene through weak van der waals' forces (Fig. 4a). From the TEM images of Fig. 4f and Fig. 4g, the surface of graphene was uniformly covered by distributed $[Fe(Htrz)_2(trz)](BF_4)$ NPs with slight conglomeration. Apparently, the distribution of SCO nanoparticles on the surface of graphene was denser in SCO-G1 than SCO-G2, and there was less large vacancy observed on graphene in SCO-G1. In addition, the conglomeration were much

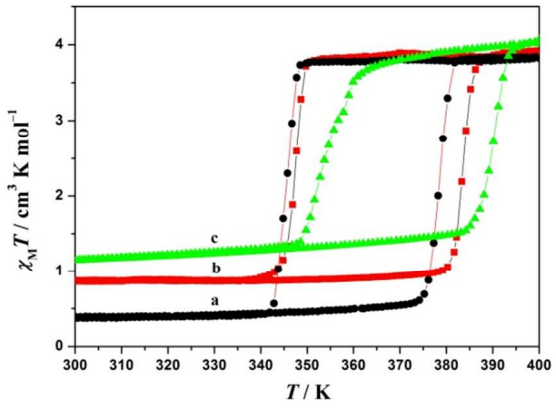

Fig. 6 Plots of $\chi_M T$ versus T for $[Fe(Htrz)_2(trz)](BF_4)$ (a, black circles), SCO-G1 (b, red squares), SCO-G2 (c, green triangles).

less in SCO-G2 than SCO-G1, indicating the degree of aggregations depended on the mass ratio of SCO NPs to graphene. All the results further demonstrated that integration of two-dimensional graphene with large surface areas and the highly dispersed SCO NPs had been successfully achieved.

Differential scanning calorimeter (DSC) was performed to check the spin-crossover phase transition temperatures in the heating mode $T_c\uparrow$ and cooling mode $T_c\downarrow$. As shown in the DSC curves of Fig. 5, $T_c\uparrow$ and $T_c\downarrow$ were 378.3 K and 345.3 K for the pure $[Fe(Htrz)_2(trz)](BF_4)$ NPs, 383.2 K and 347.5 K for SCO-G1, and 389.8 K and 351.3 K for SCO-G2, respectively. It is obvious that the phase transition temperatures of SCO-G nanocomposites shifted, where $T_c\uparrow$ and $T_c\downarrow$ moved to the higher temperatures about 4.9 K and 2.2 K for SCO-G1, and 11.5 K and 6.0 K for SCO-G2, respectively. The primary DSC results indicated that the presence of graphene influenced the phase transition temperatures of the $[Fe(Htrz)_2(trz)](BF_4)$ nanoparticles.

To confirm the effect of graphene on the spin-crossover properties, the magnetic susceptibilities were measured over the temperature range 300–400 K. As shown in Fig. 6, the SCO phenomenons were clearly preserved in the SCO NPs and SCO-G nanocomposites. At 400 K, the $\chi_M T$ values were 3.82, 3.92, and 4.01 cm^3 K mol^{-1} for $[Fe(Htrz)_2(trz)](BF_4)$, SCO-G1 and SCO-G2, respectively. The $\chi_M T$ values were in well agreement with the expected value for an iron (II) ion in the high spin (HS) state. However, the remnant HS ratios at 300 K for SCO-G1 (22.4%) and SCO-G2 (28.7%) nanocomposites were relatively higher than that of the pure $[Fe(Htrz)_2(trz)](BF_4)$ NPs (10.3%). The difference of remnant HS of SCO-G1 and SCO-G2 might be attributed to the different degrees of aggregations of SCO nanoparticles which leading to the different surface areas of the SCO polymers on the surface of graphene. It suggested that the lower aggregations of SCO NPs provided the higher surface area, while the surface Fe(II) ions of SCO NPs could favour the HS state at any temperature.[16] The spin-crossover behaviour in $[Fe(Htrz)_2(trz)](BF_4)$ NPs revealed a very abrupt and almost complete transition with a large hysteresis loop of ca. 32.5 K occurring around $T_c\uparrow$ = 378.2 K in the warming mode, and $T_c\downarrow$ = 345.7 K in the cooling mode. For SCO-G1, the spin-crossover took place with $T_c\uparrow$ = 383.3 K in the warming process, and $T_c\downarrow$ = 347.7 K in the cooling process with a thermal hysteresis of 35.6 K. For SCO-G2, the transition in warming and cooling process appeared at about $T_c\uparrow$ = 389.9 K and $T_c\downarrow$ = 351.6 K, so that the hysteresis loop was 38.3 K. The spin-crossover behavior of SCO-G nanocomposites showed the mass ratio dependent effect. With the SCO/G mass ratio decreasing, the transition was less abrupt, but both $T_c\uparrow$ and $T_c\downarrow$ moved to the higher temperatures, and the thermal hysteresises increased. The observed transition temperatures were in well agreement with those deduced from DSC measurements. The shifts of both $T_c\uparrow$ and $T_c\downarrow$ toward the higher temperatures might rise for two main reasons: fristly, the interaction between SCO NPs strengthened by the aggregations might increase the synergy of magnetic transition; secondly, the presence of interactions between the $[Fe(Htrz)_2(trz)](BF_4)$ NPs and graphene might slow down the spin transition of some amounts of iron(II) centers.[16, 17]

In summary, we have demonstrated a facile and efficient chemical approach to synthesize high-quality $[Fe(Htrz)_2(trz)](BF_4)$-graphene nanocomposites. This approach enabled a good distribution of spin-crossover NPs without further functionalization onto the surface of graphene with well controllable merit in reactant ratio and scalable advantage. SCO-G nanocomposites presented a novel platform for the construction of devices, and interesting prospect toward applications in molecular nanospintronics. It will be valuable for further investigation of other SCO nanocomposites and their potential applications in different fields.

This work was supported by the National Natural Science Foundation of China (21101078 and 21276105), the Program for New Century Excellent Talents in University of China (NCET-11-0657), the Natural Science Foundation of Jiangsu Province (BK2011143), the Fundamental Research Funds for the Central Universities (JUSRP51314B), and the Ministry of Education and the State Administration of Foreign Experts Affairs for the 111 Project (B13025).

Notes and references

[a] *School of Chemical and Material Engineering, Jiangnan University, Wuxi 214122, P. R. China. Fax: +86 510 85917763; Tel: +86 510 85917090; E-mail: zhiguogu@jiangnan.edu.cn.*
[b] *The Key Laboratory of Food Colloids and Biotechnology, Ministry of Education, School of Chemical and Material Engineering, Jiangnan University, Wuxi 214122, P. R. China*

† Electronic Supplementary Information (ESI) available: the experimental section. See DOI: 10.1039/b000000x/

1 (*a*) P. Gütlich, A. Hauser and H. Spiering, *Angew. Chem., Int. Ed.*, 1994, **33**, 2024-2054; (*b*) P. Gütlich and H. A. Goodwin (Eds.), *Spin Crossover in Transition Metal Compounds, in: Topics in Current Chemistry*, Springer, Berlin, 2004, vol. I–III; (*c*) M. A. Halcrow, *Chem. Soc. Rev*., 2011, **40**, 4119-4142; (*d*) M. A. Halcrow, (Eds.), *Spin-Crossover Materials: Properties and Application*, John Wiley & Sons, 2013; (*e*) J. Tao, R. J. Wei, R. B. Huang and L. S. Zheng, *Chem. Soc. Rev.*, 2012, **41**, 703–737.

2 (*a*) J. A. Real, A. B. Gaspar, V. Niel and M. C. Munoz, *Coord. Chem. Rev*., 2003, **236**, 121-141; (*b*) A. B. Gaspar, V. Ksenofontov, M. Seredyuk and P. Gütlich, *Coord. Chem. Rev*., 2005, **249**, 2661-2676; (*c*) Cannizzo, A. Milne, C. J. Consani, C. Gawelda, W. Bressler, Ch. van Mourik and F. Chergui, M. *Coord. Chem. Rev*., 2010, **254**, 2677-2686; (*d*) O, Sato, J. Tao and Y. Z. Zhang, *Angew. Chem., Int. Ed.*, 2007, **46**, 2152-2187; (*e*) P. Guionneau, *Dalton Trans.*, 2014, **43**, 382-393.

3 (*a*) O. Kahn and C. J. Martinez, *Science*, 1998, **279**, 44-48; (*b*) G. Aromi, L. A. Barrios, O. Roubeau and P. Gamez, *Coord. Chem. Rev*.,

2011, **255**, 485; (*c*) O. Roubeau, *Chem. Eur. J.*, 2012, **18**, 15230; (*d*) L. G. Lavrenova and O. G. Shakirova, *Eur. J. Inorg. Chem.*, 2013, 670; (e) S. Titos-Padilla, J. M. Herrera, X. W. Chen, J. J. Delgado and E. Colacio, *Angew. Chem. Int. Ed.*, 2011, **50**, 3290-3293.

4 (*a*) W. B. Lin, J. W. Rieter, Taylor and M. L. Kathryn, *Angew. Chem., Int. Ed.*, 2009, **48**, 650-658; (*b*) A. Bousseksou, G. Molnár, L. Salmon and W. Nicolazzi, C*hem. Soc. Rev.*, 2011, **40**, 3313; (*c*) M. Cavallini, *Phys. Chem. Chem. Phys.*, 2012, **14**, 11867; (*d*) H. J. Shepherd, G. Molnar, W. Nicolazzi, L Salmon and A. Bousseksou, *Eur. J. Inorg. Chem*., 2013, 653–661; (*e*) G. Molnar, L. Salmon, W. Nicolazzi, F. Terki and A. Bousseksou, *J. Mater. Chem. C.*, 2014, **2**, 1360-1366.

5 (*a*) E. Coronado, J. R. Galan-Mascaros, M. Monra-bal-Capilla, J. Garcia-Martinez and P. Pardo-Ibanez, *Adv. Mater.*, 2007, **19**, 1359-1361; (*b*) L. Joulia, S. Lionel, G. Yannick, T. Alexei, M. Karine, M. Gabor and B. Azzdeine, *Angew. Chem., Int. Ed.*, 2008, **47**, 8236-8240; (c) F. Prins, M. Monrabal-Capilla, E. A. Osorio, E. Coronado and H. S. J. van der Zant, *Adv. Mater.*, 2011, **23**, 1545–1549; (*d)* C. M. Quintero, I. A. Gural'skiy, L. Salmon, G. Molnár, C. Bergaud and A. Bousseksou, *J. Mater. Chem.*, 2012, **22**, 3745–3751; (*e*) A. Akou, I. A. Gural'skiy, L. Salmon, C. Bartual-Murgui, C. Thibault, C. Vieu, G. Molnár and A. Bousseksou, *J. Mater. Chem.*, 2012, **22**, 3752–3757.

6 (*a*) T. Forestier, S. Mornet, N. Daro, T. Nishihara, S. I. Mouri, K. Tanaka, O. Fouche, E. Freysz and J. F. Letard, *Chem. Commun.*, 2008, 4327-4329; (*b*) J. Larionova, L. Salmon, Y. Guari, A. Tokarev, K. Molvinger, G. Molnar and A. Bousseksou, *Angew. Chem., Int. Ed.*, 2008, **47**, 8236-8240; (*c*) T. Forestier, A. Kaiba, S. Pechev, D. Denux, P. Guionneau, C. Etrillard, N. Daro, E. Freysz and J. F. Letard, *Chem. Eur. J.*, 2009, **15**, 6122-6130; (*d*) Y. Chen, J. G. Ma, J. J. Zhang, W. Shi, P. Cheng, D. -Z. Liao and S. -P. Yan, *Chem. Commun.*, 2010, **46**, 5073-5075; (*e*) V. Martinez, I. Boldog, A. B. Gaspar, V. Ksenofontov, A. Bhattacharjee, P. Gutlich and J. A. Real, *Chem. Mater.*, 2010, **22**, 4271-4281; (*f*) S. Titos-Padilla, J. M. Herrera, X. W. Chen, J. J. Delgado and E. Colacio, *Angew. Chem., Int. Ed.*, 2011, **50**, 3290-3293; (*g*) C. Faulmann, J. Chahine, I. Malfant, D. de Caro, B. Cormary and L. Valade, *Dalton Trans.*, 2011, **40**, 2480-2485.

7 (*a*) A. K. Geim and K. S. Novoselov, *Nat. Mater.*, 2007, **6**, 183-191; (*b*) S. Park and R. S. Ruoff, *Nat. Nanotechnol.*, 2009, **4**, 217-224; (*c*) C. N. R. Rao, A. K. Sood, K. S. Subrahmanyam and A. Govindaraj, *Angew. Chem., Int. Ed.*, 2009, **48**, 7752-7777; (*d*) A. K. Geim, *Science*, 2009, **324**, 1530-1534; (*e*) K. P. Loh, Q. Bao, P. K. Ang and J. Yang, *J. Mater. Chem.*, 2010, **20**, 2277-2289; (*f*) H. X. Chang and H. K. Wu, *Adv. Funct. Mater.,* 2013, **23**, 1984-1997; (*g*) K. Yang, L. Feng, X. Shi and A. Liu, *Chem. Soc. Rev.*, 2013, **42**, 530-547.

8 M. D. Stoller; S. J. Park, Y. W. Zhu, J. H. An and R. S. Ruoff, *Nano Lett.* , 2008, **8**, 3498-3502.

9 (*a*) C. S. Shan, H. F. Yang, D. X. Han, Q. X. Zhang, A. Ivask and L. Niu, *Biosens. Bioelectron.*, 2010, **25**, 1070-1074; (*b*) K. Wang, Q. Liu, Q. M. Guan, J. Wu, H. N. Li and J. J. Yan, *Biosens. Bioelectron.,* 2011, **26**, 2252-2257.

10 (*a*) I. V. Lightcap and P. V. Kamat, *Acc. Chem. Res.*, 2013, **46**, 2235-2243; (*b*) C. Z Zhu and S. J. Dong, *Nanaoscale*, 2013, **5**, 10765-10775; (*c*) J. H. Zhu, M. J. Chen, Q. L. He, L. Shao, S. Y. Wei and Z. H. Guo, *RSC Adv.*, 2013, **3**, 22790-22824; (*d*) H. X. Chang and H. K. Wu, *Energy Environ. Sci.*, 2013, **6**, 3483-3507; (*e*) D. Haag·and H. H. Kung, *Top Catal*, 2014, **57**, 762-773.

11 (*a*) D. Farrusseng, S. Aguado and C. Pinel, A*ngew. Chem. Int. Ed.*, 2009, **48**, 7502-7513; (*b*) Corma, H. Carcía and F. X. L. i Xamena, *Chem. Rev*, 2010, **110**, 4606-4655; (*c*) J. R. Li, Y. G. Ma, M. C. McCarthy, J. Sculley, J. M. Yu, H. K. Jeong, P. B. Balbuena and H. C. Zhou, C*hem. Soc. Rev.*, 2011, **255**, 1791-1823; (*d*) J. Gascon, A. Corma, F. Kapteijn and F. X. L. i Xamena, *ACS Catal.*, 2014, **4**, 361-378; (*e*) Z. Y. Gu, J. Park, A. Raiff, Z. W. Wei and H. C. Zhou, *ChemCatChem*, 2014, **6**, 67-75;

12 (*a*) A. Urakawa, W. Van Beek, M. Monrabal-Capilla, J. R. Galan-Mascaros, L. Palin and M. Milanesio, *J. Phys. Chem. C.*, 2011, **115**, 1323-1329; (*b*) P. Durand, S. Pillet, E. Bendeif, C. Carteret, M. Bouazaoui, H. E. Hamzaoui, B. Capoen, L. Salmon, S. Hébert, J. Ghanbaja, L. Aranda and D. Schaniel, *J. Mater. Chem. C.*, 2013, **1**, 1933-1942; (*c*) A. Grosjean, P. Négrier, P. Bordet, C. Etrillard, D. Mondieig, S. Pechev, E. Lebraud, J. F. Létard and P. Guionneau, *Eur. J. Inorg. Chem.*, 2013, 796-802.

13 C. N. R. Rao, K. Biswas, K. S. Subrahmanyam and A. Govindaraj, *J. Mater. Chem.*, 2009, **19**, 2457-2469.

14 (*a*) F. Tuinstra and J. L. Koenig, *J. Chem. Phys.*, 1970, **53**, 1126-1130; (*b*) K. N. Kudin, B, Ozbas, H. C. Schniepp, R. K. Prud'homme, I. A. Aksay and R. Car, *Nano. Lett*., 2008, **8**, 36-41.

15 (*a*) Y. Zhou, Q. L. Bao, L. A. L. Tang, Y. L. Zhong and K. P. Loh, *Chem. Mater.*, 2009, **21**, 2950-2956; (*b*) S. R. Dhakate, N. Chauhan, S. Sharma and R. B. Mathur, *Carbon.*, 2011, **49**, 4170–4178; (*c*) S.Mikhailov (Eds.), *Physics and Applications of Graphene: Experiments*, Intech, 2011, 439-454. (*d*) A. Eckmann, A. Felten, A. Mishchenko, L. Britnell, R. Krupke, K. S. Novoselov and C. Casiraghi, *Nano Lett.*, 2012, **12**, 3925-3930; (*e*) A. C. Ferrari and D. M. Basko, *Nat. Nanotechnol.*, 2013, **8**, 235-246; (*f*) C. N. R. Rao, K. Biswas, K. S. Subrahmanyam and A. Govindaraj, *J. Mater. Chem.*, 2009, **19**, 2457-2469.

16 (*a*)A. Rotaru, I. A. Gural´skiy, G. Molnár, L. Salmon, P. demont and A. Bousseksou, *Chem. Commun.*, 2013, **48**, 4163; (*b*) J. R. Galán-Mascarós, E. Coronado, A. Forment-Aliage, M. Monrabal-Capilla, E. Pinilla-cienfuegos and M. Ceolin, *Inorg. Chem.*, 2010, **49**, 5706-5714.

17 T. Miyamachi, M. Gruber, V. Davesne, M. Bowen, S. Boukari, L. Joly, F. Scheurer, G. Rogez, T. K. Yamada, P. Ohresser, E.Beaurepaire and W. Wulfhekel, *Nature Commun.*, 2012, **3**, 938.